Cutting edge: unconventional CD8+ T cell recognition of a naturally occurring HLA-A*02:01-restricted 20mer epitope

Meeuwsen, M.H.; Wouters, A.K.; Hagedoorn, R.S.; Kester, M.G.D.; Remst, D.F.G.; Steen, D.M. van der; ... ; Heemskerk, M.H.M.

Cutting Edge

The Journal of Immunology

Cutting Edge: Unconventional CD8$^+$ T Cell Recognition of a Naturally Occurring HLA-A*02:01–Restricted 20mer Epitope

Miranda H. Meeuwsen,* Anne K. Wouters,* Renate S. Hagedoorn,* Michel G. D. Kester,* Dennis F. G. Remst,* Dirk M. van der Steen,* Arnoud de Ru,† Peter A. van Veelen,† Jamie Rossjohn,‡,§,¶ Stephanie Gras,‡,§,1 J. H. Frederik Falkenburg,* and Mirjam H. M. Heemskerk*

Unconventional HLA class I–restricted CD8$^+$ T cell epitopes, longer than 10 aa, have been implicated to play a role in human immunity against viruses and cancer. T cell recognition of long peptides, centrally bulging from the HLA cleft, has been described previously. Alternatively, long peptides can contain a linear HLA-bound core peptide, with a N- or C-terminal peptide "tail" extending from the HLA peptide binding groove. The role of such a peptide "tail" in CD8$^+$ T cell recognition remains unclear. In this study, we identified a 20mer peptide (FLPTPEELGLLGPPRPQVLA [FLP]) derived from the IL-27R subunit α gene restricted to HLA-A*02:01, for which we solved the crystal structure and demonstrated a long C-terminal "tail" extension. FLP-specific T cell clones demonstrated various recognition modes, some T cells recognized the FLP core peptide, while for other T cells the peptide tail was essential for recognition. These results demonstrate a crucial role for a C-terminal peptide tail in immunogenicity. ***The Journal of Immunology*****, 2022, 208: 1–6.**

Human leukocyte Ag class I–presented peptide epitopes are key components of CD8$^+$ T cell responses to pathogens and in cancer through recognition of neoepitopes. HLA-I complexes present peptides derived from cellular proteins on the cell surface. HLA-I peptide complexes are formed in the endoplasmic reticulum (ER), where HLA-I single chains and β_2-microglobulin (β_2m) assemble and incorporate peptides present in the ER. The ER peptide reservoir is mainly composed of peptides derived from cytosolic protein degradation by the proteasome, which are subsequently transported into the ER through peptide transporter TAP; TAP preferentially binds peptides of 8–16 aa in length (1). Besides this classical pathway, peptides can end up in the ER, independent of TAP transport, through alternative peptide processing pathways (2). For example, the C-terminal tail of type II transmembrane proteins, which is located inside the ER lumen, can be cleaved by signal peptide peptidase releasing C-terminal peptides into the ER (3). After localization into the ER, either through TAP or via alternative pathways, peptides are available for binding to HLA. Once binding to HLA has occurred, peptide–HLA (pHLA) complexes are transported to the cell surface, where recognition by T cells can take place. The HLA-I peptide binding groove contains six pockets (A–F), of which the B and F pockets typically bind the N- and C-terminally located anchor residues of peptides, respectively (4). Conventional peptides bind the B pocket through the amino acid residue at position 2 (p2) and the F pocket with the last residue pΩ. The HLA-I peptide binding groove is flanked by closed A and F pockets, generally limiting the length of binding peptides and resulting in preferential presentation of canonical peptides of 8–11 aa in length. Longer peptides can fit in HLA through binding of both anchor residues while bulging out of the groove in the center of the peptide or adapting a zigzag conformation (5). In addition, the C-terminal part of unconventional long peptides can protrude through the closed F pocket, resulting in a conventionally bound core peptide with a solvent-exposed C-terminal "tail" hanging from the groove (6, 7). Moreover, N-terminal peptide tails extending from the A pocket have been described (8). Mass spectrometry–based

*Department of Hematology, Leiden University Medical Center, Leiden, the Netherlands; †Center for Proteomics and Metabolomics, Leiden University Medical Center, Leiden, the Netherlands; ‡Infection and Immunity Program, Biomedicine Discovery Institute, Monash University, Clayton, Victoria, Australia; §Australian Research Council Centre of Excellence for Advanced Molecular Imaging, Monash University, Clayton, Victoria, Australia; and ¶Institute of Infection and Immunity, Cardiff University School of Medicine, Cardiff, United Kingdom

[1]Current address: Department of Biochemistry and Chemistry, La Trobe Institute for Molecular Science, La Trobe University, Bundoora, Victoria, Australia.

ORCIDs: 0000-0001-9268-3141 (M.H.M.); 0000-0001-9861-7276 (A.K.W.); 0000-0002-8960-7348 (M.G.D.K.); 0000-0002-7898-9408 (P.A.v.V.); 0000-0002-2020-7522 (J.R.); 0000-0001-7416-038X (S.G.); 0000-0001-6320-9133 (M.H.M.H.).

Received for publication January 5, 2022. Accepted for publication February 16, 2022.

This work was supported by KWF Dutch Cancer Society (Amsterdam, the Netherlands) Grant KWF UL-2014-6831.

The model presented in this article has been submitted to the Protein Data Bank under accession number 7T5M.

Address correspondence and reprint requests to Miranda H. Meeuwsen and Mirjam H. M. Heemskerk, Department of Hematology, Leiden University Medical Center, Leiden, the Netherlands. E-mail addresses: m.h.meeuwsen@lumc.nl (M.H.M.) and m.h.m.heemskerk@lumc.nl (M.H.M.H.)

The online version of this article contains supplemental material.

Abbreviations used in this article: Ala, alanine; ER, endoplasmic reticulum; FLP, FLPTPEELGLLGPPRPQVLA; HLA-I, HLA class I; IL-27RA, IL-27R subunit α; LCL, EBV-transformed B lymphoblastic cell line; β_2M, β_2-microglobulin; pHLA, peptide–HLA; Td, transduced.

studies revealed that unconventional long peptides compose around 5–10% of the HLA-I peptide repertoire (9–12). In addition to their relatively high abundance, T cell recognition of multiple long peptides has been described to play a role in viral and antitumor T cell immunity (13–16).

Previously, a large set of TCR–pHLA crystal structures was reviewed and demonstrated the general consensus of TCR docking on canonical pHLA complexes (17, 18). In the reported TCR–pHLA-I complexes the TCRs were oriented in a 37–90-degree angle over the peptide binding groove, with the variable domain of the TCRα-chain generally located over the α2 helix and the TCRβ-chain over the α1 of the HLA molecule. The three loops located at the membrane-distal end of both TCR chains contain CDR1, CDR2, and CDR3. CDR1 and CDR2 (encoded by the germline variable [V] gene) interact primarily with the HLA molecule, while the hypervariable CDR3 domain binds to the peptide and HLA molecule.

Longer peptides usually bulge centrally from the peptide binding cleft (5). Bulged peptides were described to be recognized through varying TCR docking mechanisms. Rigid peptide bulges maintain their original conformation upon TCR ligation, while more motile bulges can be flattened upon TCR interaction (16, 19–21). T cells recognizing bulged long peptides were shown to engage with the core of the peptide bulging out of the HLA groove. In contrast, it is unknown how N- or C-terminal peptide tails extending from HLA cleft impact T cell recognition. To gain insight into the role of the peptide tail in the interaction with $CD8^+$ T cells, we investigated HLA binding of a naturally occurring 20mer peptide FLPTPEELGLLGPPRPQVLA (referred to as FLP) derived from the IL-27R subunit α (IL-27RA) protein presented in HLA-A*02:01 (HLA-A2). We solved the crystal structure of the HLA-A2-FLP complex and revealed that only the first 11 aa of the peptide bound in the HLA-A2 binding groove (FLPTPEELGLL), while a proline-rich solvent exposed a C-terminal tail of nine residues (GPPRPQVLA) extending from the F pocket of the HLA-A2 molecule. T cells recognizing the FLP peptide revealed that part of the C-terminal "tail" can be critical for T cell recognition, providing new insight in the diversity of T cells recognizing unconventional long peptides in HLA-I.

Materials and Methods

Peptide identification

HLA-I peptidomes of $HLA\text{-}A2^+$ EBV-transformed B lymphoblastic cell lines (LCLs) LCL-HHC and LCL-JYW were previously determined by peptide elution and mass spectrometry analysis (22). Peptide length variation was assessed for peptides containing anchor residues for binding to expressed HLA-I alleles (9). In this study, pHLA monomers containing 20mer peptide FLP derived from the IL-27RA in HLA-A2 were folded and used to generate pHLA tetramers as previously described by Hassan et al. (9). Peptides were synthesized by standard Fmoc chemistry and dissolved in DMSO.

Protein expression, purification, crystallization, and structure determination

DNA plasmids encoding HLA-A2 α-chain (1–275) and human β_2m were transformed separately into a BL21 strain of *Escherichia coli*. Recombinant proteins were expressed insoluble as inclusion bodies, extracted, and purified. Soluble pHLA complex was produced by refolding 30 mg HLA-A2 α-chain, 5 mg β_2m, and 5 mg FLP peptide in a 0.5 l buffer of 3 M urea, 0.5 M L-arginine, 0.1 M Tris–HCl (pH 8.0), 2.5 mM EDTA (pH 8.0), 5 mM glutathione (reduced), and 1.25 mM glutathione (oxidized). The mixture was stirred at 4°C for 3 h and dialyzed against 10 L of 10 mM Tris–HCl (pH 8.0) three times over a 24-h period (23). Soluble pHLA was purified using anion exchange chromatography using a HiTrapQ column. The HLA-A2-FLP complex was crystallized using a vapor diffusion method with a 1:1 ratio of protein/mother liquor. The protein was 5 mg/ml in 0.1 M Tris–HCl (pH 8) and 0.15 M NaCl, and the mother liquor was composed of a mixture of 0.12 M monosaccharides (D-glucose; D-mannose; D-galactose; L-fucose; D-xylose; *N*-acetyl-D-glucosamine), 0.1 M Na-HEPES and MOPS buffer at pH 7.5, 20% w/v glycerol, and 10% w/v PEG 4000. The crystals were flash frozen in liquid nitrogen, and data were collected upon the MX1 beamline at the Australian Synchrotron, part of ANSTO, Australia (24). The data were processed using XDS (25), and the structure was determined by molecular replacement using the PHASER program (26) from the CCP4 suite (27) with a model of HLA-A2 without peptide [derived from the Protein Data Bank 3GSC (28)]. Manual model building was conducted using COOT (29), followed by refinement with BUSTER (30). The final model has been validated and deposited using the Worldwide Protein Data Bank OneDep System with accession code: 7T5M. The final refinement statistics are summarized in Supplemental Table I. All molecular graphics representations were created using PyMOL.

T cell isolation

PBMCs were isolated from buffy coats obtained from HLA-A2–negative healthy donors after written informed consent according to the Declaration of Helsinki. pHLA-$tetramer^+$ $CD8^+$ T cells were enriched, single cell sorted, and clonally expanded as previously described (9). FLP-A2 specificity was determined by pHLA-tetramer stain.

Target cell generation

T2 and Raji cells were transduced (Td) with IL-27RA in a MP71-IRES-NGFR vector. Td cells were purified for transgene expression by MACS before use in experiments. Raji cells were additionally Td with HLA-A2 in a pLZRS-markerless vector and purified.

T cell assay

T cell stimulation assays were performed by overnight incubation of 5000 T cells with 30,000 target cells in 384-well plates. For peptide recognition, target cells were loaded with 100 nM peptide or decreasing concentrations starting at 1 μM in peptide titration experiments. IFN-γ production was measured by ELISA. C-terminal length variants of FLP peptide were generated. Purity of all length variants was confirmed by HPLC and mass spectrometry. FLP 15mer peptide was used for alanine (Ala) scanning, and all amino acids were separately substituted by an Ala.

Quantitative RT-PCR

IL27RA expression was measured by quantitative RT-PCR as previously described (31). Gene expression was calculated relative to the average expression of housekeeping genes: *GUSB*, *PSMB4*, and *VPS29*.

Results and Discussion

Identification of an HLA-A2 binding 20mer peptide

In a previous study, we mapped the HLA-I peptidome of LCLs by peptide elution followed by mass spectrometry (9, 22). HLA-I peptides were eluted using W6/32 Ab followed by selection of peptides containing anchor residues for HLA-I. This study revealed that HLA-I–presented peptides longer than 11 aa occur more frequently than previously anticipated. In this study, we investigated HLA binding and T cell recognition of 20mer peptide FLP identified by Hassan et al. (9, 22), which originated from the C-terminal end of the IL-27RA protein. The FLP peptide was eluted from $HLA\text{-}A2^+$ LCL-HHC, but not from $HLA\text{-}A2^+$ LCL-JYW (Fig. 1). The FLP peptide contains

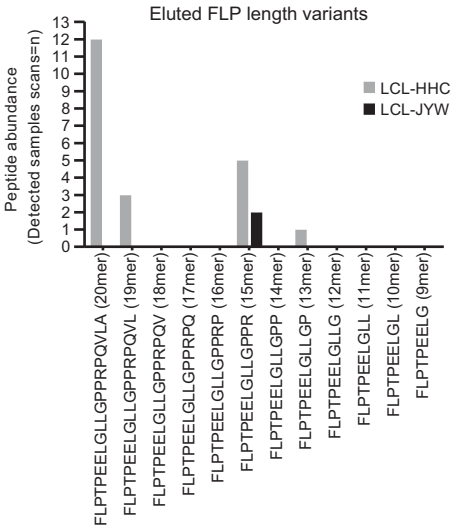

FIGURE 1. Identification of IL-27RA–derived length variants of FLP peptide from HLA-A2$^+$ LCLs. HLA-I–presented peptides were eluted from 40 × 10^9 HLA-A2$^+$ LCLs and measured by mass spectrometry. Length variants of FLP peptides derived from the IL-27RA protein were identified. Shown are frequencies of detection, determined by number of detected sample scans of FLP length variant from LCL-HHC (in grey) and LCL-JYW (in black).

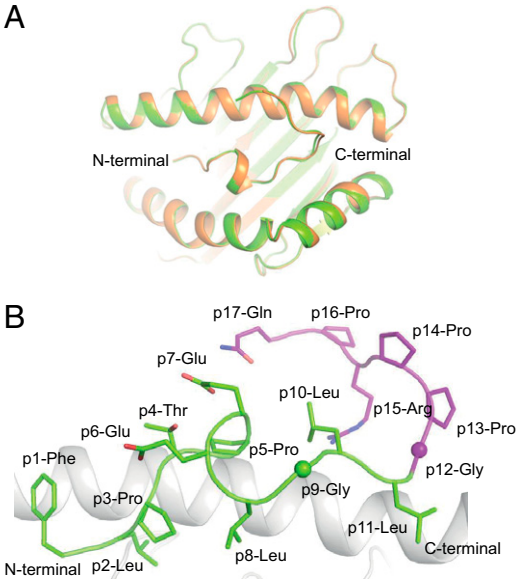

FIGURE 2. Crystal structure of the HLA-A2–FLP complex. (**A**) Superposition of the two HLA-A2–FLP complexes present in the asymmetric unit represented as a cartoon in green and orange. (**B**) Structure of the FLP-20mer peptide (cartoon and stick) in the cleft of HLA-A2 (white cartoon). The first 11 residues of the FLP-20mer peptide colored in green are bound to the Ag binding cleft, while the C-terminal tail (purple) is coming out of the cleft.

multiple potential anchor residues that suggest binding to HLA-A2. For example, the leucine at p2 could act as the p2 anchor residue for binding to HLA-A2. Alternatively, in case of an unconventional N-terminal peptide tail extending from the HLA groove, leucine at p8, p10, or p11 could act as the p2 anchor residue. In addition, the C-terminal pΩ anchor residue could be the leucine at p10, p11, or p19, as well as the valine at p18. Stable binding of FLP to HLA-A2 was confirmed by successful refolding and crystallization of the HLA-A2–FLP complex.

Crystal structure of HLA-A2–FLP revealed the presence of a long C-terminal "tail"

To investigate how the FLP peptide was presented by the HLA-A2 molecule, we solved the crystal structure of the HLA-A2–FLP complex at 1.7-Å resolution (Supplemental Table I). The crystal structure contains two molecules in the asymmetric unit. The superposition of the two pHLA complexes revealed that they both adopted the same conformation, with a root mean square of 0.23 Å for the Ag binding cleft and 0.34 Å for the peptide (Fig. 2A). Therefore, the structural analysis was performed with one of the complexes. The HLA-A2–FLP structure revealed that amino acids at p1–p11 bind in the HLA-A2 peptide binding groove in the same manner as conventional HLA-I–presented peptides, with p11-L as the pΩ anchor residue (Fig. 2B). Amino acids p12–p20 extend from the F pocket and form a solvent-exposed C-terminal "tail." Part of the peptide tail (p12–p17) was clearly defined in the electron density (Supplemental Fig. 1A, 1B), while the electron density was weak for C-terminal residues (p18–p20), indicating high flexibility of this part. The proline-rich nature of the p12–p17 extended region presumably added rigidity to this section of the peptide, thereby enabling it to be readily visualized (19).

Identification of FLP peptide-specific CD8 ± T cells revealed immunogenicity

To assess the immunogenicity of FLP peptide, we isolated T cells from HLA-A2–negative healthy donors to circumvent immunogenic tolerance for this nonmutated self-peptide (31, 32). Using HLA-A2–FLP tetramers, we successfully isolated CD8$^+$ T cell clones (Fig. 3A). These T cell clones demonstrated functional recognition of FLP peptide upon peptide titration using HLA-A2 Td Raji cells (Fig. 3B). Unloaded *IL27RA*-negative Raji cells were not recognized, showing FLP peptide specificity (Fig. 3B, Supplemental Fig. 1C).

Recognition of endogenously processed and presented FLP peptide was observed by T cells stimulated with *IL27RA*-expressing T2 cells (Fig. 3C, Supplemental Fig. 1C), indicating that the identified T cell clones were potent enough to recognize target cells naturally expressing the *IL27RA* gene. In addition, recognition of T2 cells was enhanced by retroviral overexpression of the *IL27RA* gene (Fig. 3C). Similarly, Td of IL-27RA into Raji cells induced recognition, validating the requirement for *IL27RA* expression for target cell recognition. Recognition of TAP-deficient T2 cells by FLP-specific T cell clones suggests that FLP peptide, which is located at the C-terminal end of the IL-27RA protein, is processed and presented independent of TAP transport through an alternative pathway remaining to be identified. This observation is in accordance with the overrepresentation of C-terminal peptides in the ligandome of TAP-deficient cells (33).

Finally, LCLs from donors HHC and JYW were cocultured with the T cell clones; despite similar natural *IL27RA* expression levels (Supplemental Fig. 1C), LCLs from donor HHC were recognized, while LCLs from donor JYW were not recognized (Fig. 3C). This corresponded with the difference in abundance of FLP length variants in peptide elution data of the two LCLs (Fig. 1), which demonstrated that FLP length variants, including the 20mer peptide, were abundantly present on LCL-HHC cells, whereas no 20mer peptide and only one length variant could be detected in the peptide elution data of LCL-JYW (Fig. 1). In total, length variants of FLP were identified 21 times

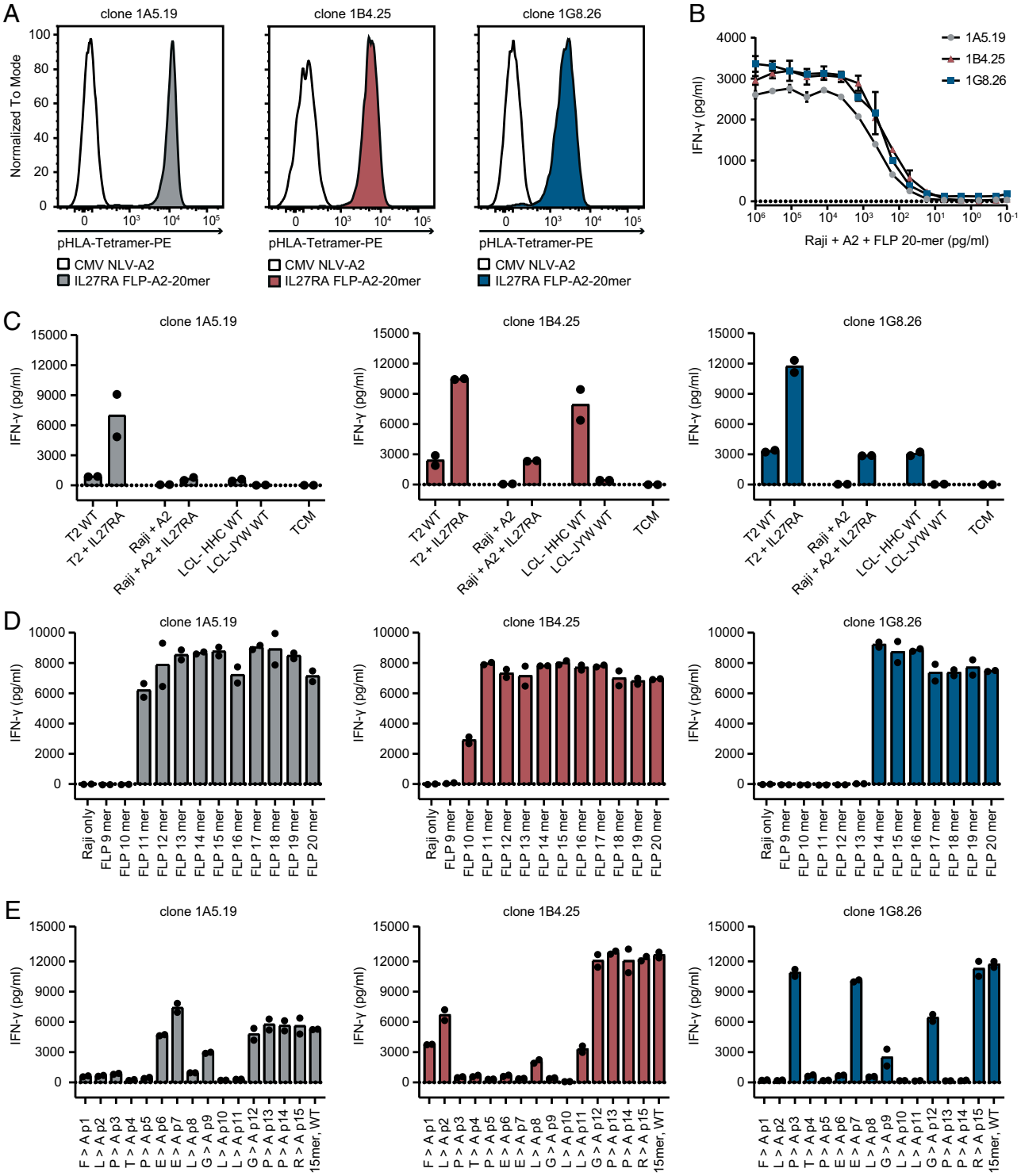

FIGURE 3. Reactivity of FLP-specific T cell clones. (**A**) T cell clones 1A5.19, 1B4.25, and 1G8.26 stained with IL-27RA FLP pHLA-tetramer-PE (gray red or blue) or control CMV NLVPMVATV (NLV) HLA-A2 tetramer (white) gated on live cells. (**B**–**E**) IFN-γ production after overnight coculture. Values represent mean of technical duplicates; data are representative examples of three experiments. (B) T cell clones cocultured with Raji cells Td with HLA-A2 loaded with decreasing FLP peptide concentrations. (C) T cell clones cocultured with Raji cells Td with HLA-A2 (Raji + A2), Raji + A2 additionally Td with the IL-27RA gene (+IL-27RA), HLA-A2$^+$ wild type (WT) T2 cells, T2 cells Td with the IL-27RA gene (+IL-27RA), HLA-A2$^+$ WT LCLs from donor HHC, HLA-A2$^+$ WT LCLs from donor JYW, and medium (TCM) only. (D) Raji + A2 loaded with 100 nM C-terminal length variants of FLP peptide. (E) Raji + A2 loaded with 100 nM Ala scan of FLP 15mer peptide.

from LCL-HHC, but only 2 times from LCL-JYW. The substantial difference in detection of FLP length variants indicated differential involvement of the pathway underlying presentation of FLP peptides in LCL-HHC and JYW.

Solvent-exposed C-terminal "tail" of FLP peptide plays a role in T cell recognition

To investigate whether the solvent-exposed "tail" of FLP peptide plays a role in T cell recognition, we loaded C-terminal

length variants of FLP on HLA-A2 Td Raji cells. Recognition by T cell clone 1A5.19 was located in the core between p1 and p11 of FLP peptide, because recognition was not influenced by length variations of the tail (p12–p20) (Fig. 3D). Recognition was lost when stimulated with FLP-10mer peptide, demonstrating the requirement for the p11-L anchor residue to be present that would likely conserve the same core structure as the 20mer peptide. T cell clone 1B4.25 demonstrated a comparable recognition pattern but additionally recognized FLP-10mer peptide at a reduced level (Fig. 3D), indicating that p10-L could act as an alternative, but less efficient, anchor residue. Finally, T cell clone 1G8.26 recognized FLP 20-14mer peptides to the same extent as FLP-20mer peptide, but recognition was abrogated upon stimulation with FLP-13mer or shorter peptides (Fig. 3D). Therefore, the proline at p14 played an essential role in recognition by this T cell clone, demonstrating that the proximal part of the C-terminal peptide "tail" was involved in T cell recognition. For all T cell clones, no differences were observed between recognition of FLP-20mer and FLP-15mer, indicating that p15-p20 did not influence T cell recognition. To confirm that amino acids in the proximal part of the "tail" are important for recognition by T cell clone 1G8.26, we generated and loaded an Ala scan of FLP-15mer onto HLA-A2 Td Raji cells. For T cell clones 1A5.19 and 1B4.25, Ala substitutions between p12 and p15 did not influence recognition of the FLP peptide, whereas recognition by T cell clone 1G8.26 was abrogated when p13 and p14 were replaced by Ala, confirming the previously observed role of the proximal part of the peptide tail for recognition by this clone (Fig. 3E). In addition, Ala substitutions between p1 and p11 demonstrated that all three clones recognized the core region of the peptide but exhibited differential recognition patterns of the FLP pHLA-A2 complex. Thus, T cell clone 1G8.26 recognized the core, as well as the tail region, of the FLP peptide, while clones 1A5.19 and 1B4.25 recognized the core peptide alone. The combined recognition of the core region as well as the proximal part of the tail by clone 1G8.26 suggested that upon TCR binding, the peptide tail is oriented away from the peptide binding groove rather than being folded back over the linear peptide core, thereby allowing simultaneous TCR contact with the core, as well as the proximal part of the peptide tail.

Remesh et al. (7) previously reported that longer peptides extend at the C terminus by opening the F pocket with a charged amino acid not more than three residues after the pΩ anchor. In our study, the crystal structure of the HLA-A2-FLP complex does not reveal opening of the F pocket, and in addition the first charged amino acid at p15 was found to be irrelevant for recognition (Fig 3D, 3E), demonstrating that a C-terminal peptide tail can extend from the HLA cleft without opening of the F pocket by a charged amino acid.

To conclude, these results demonstrated immunogenicity of a 20mer peptide composed of a conventional core peptide and a C-terminal peptide tail coming out the F pocket presented in HLA-A2. One of three identified T cell clones required the peptide tail to allow peptide recognition, highlighting that the proximal part of the C-terminal peptide tail can be a crucial component of such an unconventional T cell epitope. These results contribute to the knowledge about the dynamic range in functional T cell epitopes that exist beyond canonical peptides. The variable recognition patterns observed between T cell clones would indicate that the TCRs bind FLP through different docking modes, and further study will be required to gain a detailed understanding of the interaction between TCRs and this unconventional peptide.

Disclosures

The authors have no financial conflicts of interest.

References

1. van Endert, P. M., R. Tampé, T. H. Meyer, R. Tisch, J. F. Bach, and H. O. McDevitt. 1994. A sequential model for peptide binding and transport by the transporters associated with antigen processing. *Immunity* 1: 491–500.
2. Oliveira, C. C., and T. van Hall. 2015. Alternative antigen processing for MHC class I: multiple roads lead to Rome. *Front. Immunol.* 6: 298.
3. Oliveira, C. C., B. Querido, M. Sluijter, A. F. de Groot, R. van der Zee, M. J. Rabelink, R. C. Hoeben, F. Ossendorp, S. H. van der Burg, and T. van Hall. 2013. New role of signal peptide peptidase to liberate C-terminal peptides for MHC class I presentation. *J. Immunol.* 191: 4020–4028.
4. Nguyen, A. T., C. Szeto, and S. Gras. 2021. The pockets guide to HLA class I molecules. *Biochem. Soc. Trans.* 49: 2319–2331.
5. Josephs, T. M., E. J. Grant, and S. Gras. 2017. Molecular challenges imposed by MHC-I restricted long epitopes on T cell immunity. *Biol. Chem.* 398: 1027–1036.
6. Collins, E. J., D. N. Garboczi, and D. C. Wiley. 1994. Three-dimensional structure of a peptide extending from one end of a class I MHC binding site. *Nature* 371: 626–629.
7. Remesh, S. G., M. Andreatta, G. Ying, T. Kaever, M. Nielsen, C. McMurtrey, W. Hildebrand, B. Peters, and D. M. Zajonc. 2017. Unconventional peptide presentation by major histocompatibility complex (MHC) class I allele HLA-A*02:01: BREAKING CONFINEMENT. *J. Biol. Chem.* 292: 5262–5270.
8. Pymm, P., P. T. Illing, S. H. Ramarathinam, G. M. O'Connor, V. A. Hughes, C. Hitchen, D. A. Price, B. K. Ho, D. W. McVicar, A. G. Brooks, et al. 2017. MHC-I peptides get out of the groove and enable a novel mechanism of HIV-1 escape. *Nat. Struct. Mol. Biol.* 24: 387–394.
9. Hassan, C., E. Chabrol, L. Jahn, M. G. Kester, A. H. de Ru, J. W. Drijfhout, J. Rossjohn, J. H. Falkenburg, M. H. Heemskerk, S. Gras, and P. A. van Veelen. 2015. Naturally processed non-canonical HLA-A*02:01 presented peptides. *J. Biol. Chem.* 290: 2593–2603.
10. Hickman, H. D., A. D. Luis, R. Buchli, S. R. Few, M. Sathiamurthy, R. S. VanGundy, C. F. Giberson, and W. H. Hildebrand. 2004. Toward a definition of self: proteomic evaluation of the class I peptide repertoire. *J. Immunol.* 172: 2944–2952.
11. Mommen, G. P., C. K. Frese, H. D. Meiring, J. van Gaans-van den Brink, A. P. de Jong, C. A. van Els, and A. J. Heck. 2014. Expanding the detectable HLA peptide repertoire using electron-transfer/higher-energy collision dissociation (EThcD). *Proc. Natl. Acad. Sci. USA* 111: 4507–4512.
12. Burrows, S. R., J. Rossjohn, and J. McCluskey. 2006. Have we cut ourselves too short in mapping CTL epitopes? *Trends Immunol.* 27: 11–16.
13. Pudney, V. A., A. M. Leese, A. B. Rickinson, and A. D. Hislop. 2005. CD8+ immunodominance among Epstein-Barr virus lytic cycle antigens directly reflects the efficiency of antigen presentation in lytically infected cells. *J. Exp. Med.* 201: 349–360.
14. Tynan, F. E., N. A. Borg, J. J. Miles, T. Beddoe, D. El-Hassen, S. L. Silins, W. J. van Zuylen, A. W. Purcell, L. Kjer-Nielsen, J. McCluskey, et al. 2005. High resolution structures of highly bulged viral epitopes bound to major histocompatibility complex class I. Implications for T-cell receptor engagement and T-cell immunodominance. *J. Biol. Chem.* 280: 23900–23909.
15. Probst-Kepper, M., H. J. Hecht, H. Herrmann, V. Janke, F. Ocklenburg, J. Klempnauer, B. J. van den Eynde, and S. Weiss. 2004. Conformational restraints and flexibility of 14-meric peptides in complex with HLA-B*3501. *J. Immunol.* 173: 5610–5616.
16. Chan, K. F., B. S. Gully, S. Gras, D. X. Beringer, L. Kjer-Nielsen, J. Cebon, J. McCluskey, W. Chen, and J. Rossjohn. 2018. Divergent T-cell receptor recognition modes of a HLA-I restricted extended tumour-associated peptide. *Nat. Commun.* 9: 1026.
17. Rossjohn, J., S. Gras, J. J. Miles, S. J. Turner, D. I. Godfrey, and J. McCluskey. 2015. T cell antigen receptor recognition of antigen-presenting molecules. *Annu. Rev. Immunol.* 33: 169–200.
18. La Gruta, N. L., S. Gras, S. R. Daley, P. G. Thomas, and J. Rossjohn. 2018. Understanding the drivers of MHC restriction of T cell receptors. *Nat. Rev. Immunol.* 18: 467–478.
19. Tynan, F. E., S. R. Burrows, A. M. Buckle, C. S. Clements, N. A. Borg, J. J. Miles, T. Beddoe, J. C. Whisstock, M. C. Wilce, S. L. Silins, et al. 2005. T cell receptor recognition of a 'super-bulged' major histocompatibility complex class I-bound peptide. *Nat. Immunol.* 6: 1114–1122.
20. Tynan, F. E., H. H. Reid, L. Kjer-Nielsen, J. J. Miles, M. C. Wilce, L. Kostenko, N. A. Borg, N. A. Williamson, T. Beddoe, A. W. Purcell, et al. 2007. A T cell

receptor flattens a bulged antigenic peptide presented by a major histocompatibility complex class I molecule. *Nat. Immunol.* 8: 268–276.
21. Liu, Y. C., J. J. Miles, M. A. Neller, E. Gostick, D. A. Price, A. W. Purcell, J. McCluskey, S. R. Burrows, J. Rossjohn, and S. Gras. 2013. Highly divergent T-cell receptor binding modes underlie specific recognition of a bulged viral peptide bound to a human leukocyte antigen class I molecule. *J. Biol. Chem.* 288: 15442–15454.
22. Hassan, C., M. G. Kester, A. H. de Ru, P. Hombrink, J. W. Drijfhout, H. Nijveen, J. A. Leunissen, M. H. Heemskerk, J. H. Falkenburg, and P. A. van Veelen. 2013. The human leukocyte antigen-presented ligandome of B lymphocytes. *Mol. Cell. Proteomics* 12: 1829–1843.
23. Chatzileontiadou, D. S. M., C. Szeto, D. Jayasinghe, and S. Gras. 2021. Protein purification and crystallization of HLA-A*02:01 in complex with SARS-CoV-2 peptides. *STAR Protoc.* 2: 100635.
24. Aragão, D., J. Aishima, H. Cherukuvada, R. Clarken, M. Clift, N. P. Cowieson, D. J. Ericsson, C. L. Gee, S. Macedo, N. Mudie, et al. 2018. MX2: a high-flux undulator microfocus beamline serving both the chemical and macromolecular crystallography communities at the Australian Synchrotron. *J. Synchrotron Radiat.* 25: 885–891.
25. Kabsch, W. 2010. XDS. *Acta Crystallogr. D Biol. Crystallogr.* 66: 125–132.
26. McCoy, A. J., R. W. Grosse-Kunstleve, P. D. Adams, M. D. Winn, L. C. Storoni, and R. J. Read. 2007. Phaser crystallographic software. *J. Appl. Cryst.* 40: 658–674.
27. Collaborative Computational Project, Number 4. 1994. The CCP4 suite: programs for protein crystallography. *Acta Crystallogr. D Biol. Crystallogr.* 50: 760–763.
28. Gras, S., X. Saulquin, J. B. Reiser, E. Debeaupuis, K. Echasserieau, A. Kissenpfennig, F. Legoux, A. Chouquet, M. Le Gorrec, P. Machillot, et al. 2009. Structural bases for the affinity-driven selection of a public TCR against a dominant human cytomegalovirus epitope. *J. Immunol.* 183: 430–437.
29. Emsley, P., B. Lohkamp, W. G. Scott, and K. Cowtan. 2010. Features and development of Coot. *Acta Crystallogr. D Biol. Crystallogr.* 66: 486–501.
30. Bricogne, G., E. Blanc, M. T. Brandl, C. Flensburg, P. Keller, W. Paciorek, P. Roversi, A. Scharff, O.S. Smart, C. Vonrhein, and T.O. Womack. 2011. *Buster version 2.10.* Global Phasing Ltd., Cambridge, UK.
31. Jahn, L., D. M. van der Steen, R. S. Hagedoorn, P. Hombrink, M. G. Kester, M. P. Schoonakker, D. de Ridder, P. A. van Veelen, J. H. Falkenburg, and M. H. Heemskerk. 2016. Generation of CD20-specific TCRs for TCR gene therapy of CD20low B-cell malignancies insusceptible to CD20-targeting antibodies. *Oncotarget* 7: 77021–77037.
32. Amir, A. L., D. M. van der Steen, M. M. van Loenen, R. S. Hagedoorn, R. de Boer, M. D. Kester, A. H. de Ru, G. J. Lugthart, C. van Kooten, P. S. Hiemstra, et al. 2011. PRAME-specific Allo-HLA-restricted T cells with potent antitumor reactivity useful for therapeutic T-cell receptor gene transfer. *Clin. Cancer Res.* 17: 5615–5625.
33. Martín-Galiano, A. J., and D. López. 2019. Computational characterization of the peptidome in transporter associated with antigen processing (TAP)-deficient cells. *PLoS One* 14: e0210583.